# Performance Evaluation of Vortex Generator of Finite Thickness to Augment Heat Transfer in a Compact Heat Exchanger

***ABSTRACT***
*The effect of non dimensional thickness of a winglet type vortex generator is investigated in terms of heat transfer rate, stream-wise vortices and flow losses in a plate fin heat exchanger with triangular inserts as secondary fins. The winglet type vortex generators are mounted alternatively on the upper and lower plates of the heat exchanger to disrupt the flow in the triangular domain formed by the inserts. The fluid flow within the duct is considered to be confined and laminar. While the hydrodynamic flow is fully developed, the thermal characteristics are assumed to be in developing stage under isothermal boundary conditions. The winglet is located in the duct where the flow is fully developed (Xi = 2.765 w.r.t. leading edge) at an angle of 27$^o$ with respect to the bulk flow direction. The aforesaid performance characteristics are computed numerically by solving the mass continuity, momentum and energy equations. Computational results clearly show an enhancement of 12.91% in the heat transfer rate (quantified as $Nu_m/ Nu_o$) for an increase in non dimensional thickness c/2H from 0.00 to 0.05. Besides, the pressure drop penalty is found to be only 3.8% at Re = 150. The results have also been substantiated by carrying out experiments on a scaled model configuration. Three dimensional velocity components are verified behind the winglet to ensure the stable flow field for non dimensional thickness of winglet c/2H=0.05 and Reynolds number of 350.*

***KEYWORDS:*** *Winglet, Vortex Generator, Heat Transfer Enhancement, Plate-Fin Heat Exchanger*

## 1. INTRODUCTION

Heat exchangers are essential components for the dissemination of energy and there is a growing concern on increasing the effectiveness of new age heat exchangers. Now a days, compact heat exchangers are widely used to transfer energy in most of the industrial, commercial and domestic applications. One of the passive methods to enhance the heat transfer performance on the gas side involves the use of vortex generators which disrupt the boundary layer and churn the fluid thoroughly.

Literature shows that the study of the heat transfer enhancement by using the longitudinal vortex generator is carried out on various types of geometrical configurations. The flat plate with vortex generators attracted the interest of several researchers acrross the globe. (Torii et al. 1989) evaluated the local heat transfer enhancement with a single delta winglet mounted on a flat plate. (Turk, A.Y., Junkhan, G.H., 1986) predicted heat transfer increment using multiple rectangular winglet vortex generators at the leading edge of a flat plate. The related work has been carried out by many researchers. (Yanagihara, J.I., Torii, K., 1993) The channel flow has different properties as compared to flat plate boundary layer flow. In the former case, a favorable pressure gradient always exists and the flow becomes fully developed in the downstream which is missing in the latter. (Biswas et al. 1996) numerical & experimentlly determined the flow structure, vorticity contours confirmed the formation of main vortex, induced vortices and the corner vortex. A much higher value of (j/f) for an angle of attack of 15° was computed numerically as compared to those for 22.5°, 30°

and 37.5°. (Tiggleback et al. 1992) further compared the four basic forms of vortex generators i.e. delta wing, rectangular wing, pair of delta winglets and pair of rectangular winglets. These vortex generators were punched out from the parallel plates of the heat exchanger. Winglets performed better than the wings and a pair of delta winglet performed slightly better than the rectangular winglet at higher angles of attack and at higher Reynolds numbers. (Fiebig et al. 1998) presented a survey on triangular and rectangular protrusions in channel flows using wing and wingle type vortex genertor. Heat transfer enhancement was higher in laminar flow than in turbulent flow and for single vortex generators. (Pesteei et al. 2005) studied the location effect of the winglet on heat transfer enhancement and the pressure drop in a fin tube heat exchanger experimentally. The investigation showed an increase of around 46% in the value of average Nusselt number. (Sohankar, A., Davidson, L., 2003) attempted unsteady three-dimensional Direct Numerical Simulation (DNS) and Large Eddy Simulation (LES) of heat and fluid flow in a plate-fin heat exchanger with thick rectangular winglet type vortex generators at Reynolds and Prandtl numbers of 2000 and 0.71 respectively. (Brockmeier et al. 1993) compared the performance of a parallel plate-fin channel using delta wing vortex generators with that of four standard heat exchanger surfaces, *viz*, two plain fins, an offset strip and louvered fin geometry. For the standard surfaces, the basic performance characteristics in terms of heat transfer rate and friction data versus Reynolds number were taken from published experimental results; however, in the case of vortex generator surface, numerical prediction was done. The vortex generator surface allowed a reduction of 76% in the heat transfer surface area for fixed heat duty and for fixed pumping power

These two configurations pairing common flow-down and V pairing common flow-up were numerically investigated for the case of three-dimensional incompressible viscous flow in a rectangular channel by (Yang et al., 2001). The shape of the vortices changed to an ellipse elongated in spanwise and vertical directions for ommon flow-down and flow-up configurations respectively. (Kataoka et al., 1977) indicated that heat transfer was locally enhanced in the region where two neighboring vortices induced flow towards the heat transfer surface (downwash region). Local thinning of the boundary layer associated with the secondary flow was found to be cause of heat transfer augmentation. (Yang et al., 2008) further predicted the effects of delta winglet pair in common flow-up configuration in a rectangular channel flow. In the case of common flow-up pair, the distortion of the thermal boundary layer was not as significant as the distortion of the hydraulic boundary layer.

(Deb et al. 1995) proposed a numerical model to compute both laminar and turbulent flow through a rectangular channel containing built-in winglet vortex generators. The results confirmed the use of winglets to be a more effective augmentation technique. Numerical simulations of turbulent flows in a rectangular channel with vortex generators mounted on the bottom wall were also carried out by (Zhu et al. 1993). Enhancement in heat transfer in Plate-fin isosceles triangular ducts were investigated by (Zhang et al. 2007). Conductance of the fin from zero to infinity and convection of the fluid was also considered which made it a conjugate problem. Apex angle of the triangular inserts was varied from 30° to 120°. (Vasudevan et al. 2000) predicted numerically the heat transfer enhancement achieved using plate triangular fin heat exchanger. The work carried out to size the plate fin heat exchanger with the welded and stamped delta winglet mounted on the inclined wall of the triangular secondary fin. Around 20-25% enhancement in heat transfer rate was achieved at the expense of a

moderate pressure drop. (Sachdeva et al. 2010) presented heat transfer characteristics with with delta and rectangular wing vortex generators. This geometrical configuration was investigated for various angles of attack of the wing i.e. 15º, 20º, 26º and 37º and Reynolds numbers not exceeding 200. (Gupta et al. 2009) reported the potential of a winglet pair type vortex generator for heat transfer enhancement in a plate fin heat exchanger, with triangular fins as inserts. The computations was performed at $Re$=200 and angle of attack,  =20°. The results showed an increase of 13% in the heat transfer rate, even at the exit, with the winglet pair for varying winglet heights. (Hiravennavar et al. 2007) investigated numerically the performance of winglets with finite thickness in rectangular channel with the values of Re, aspect ratio and W/H at 790, 3.0 and 0.0622 respectively. It was concluded that spanwise average Nusselt number increases with an increase in the thickness of the winglets and it was reasoned that the finite thickness of winglet provides more cross-sectional area for energy transfer from the bottom plate and hence, results in increased heat transfer.

It can be concluded form the foregoing discussion that plate triangular fin heat exchanger has not received adequate attention. Even experimental studies on this type of compact heat exchanger with vortex generators are not available in literature. Besides, numerical investigations considering the thickness of vortex generators are also quite scarce.

## 2. PROBLEM FORMULATION

Figure 1(a) shows the geometry of the plate triangular fin heat exchanger and Figure 1(b) shows the actual model of plate triangular fin heat exchanger with delta winglets mounted on the plates in such a manner that the winglets are enclosed in the triangular duct formed by the fins.
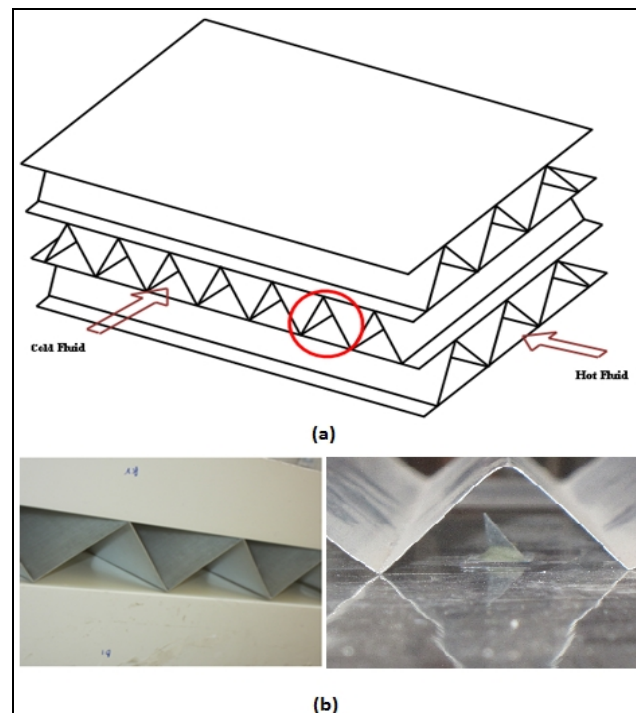


Figure 1(a) Heat Exchnger model (b) actual triangular insert of plate fin
heat exchanger without and with winglet

The working fluid considered herein is air. The elaborated view in Figure 2 shows the delta winglet on the bottom surfaces of heat exchanger plat. These fins may also act as spacers between the parallel plates of the heat exchanger. The built-in vortex generators are the protruded surfaces which can be joined by either welding or brazing. These protruded surfaces are kept at some angle with respect to the direction of fluid flow which is known as the angle of attack of the vortex generator. A two dimensional view of the shape of delta winglet mounted on plate is shown in Figure 3.
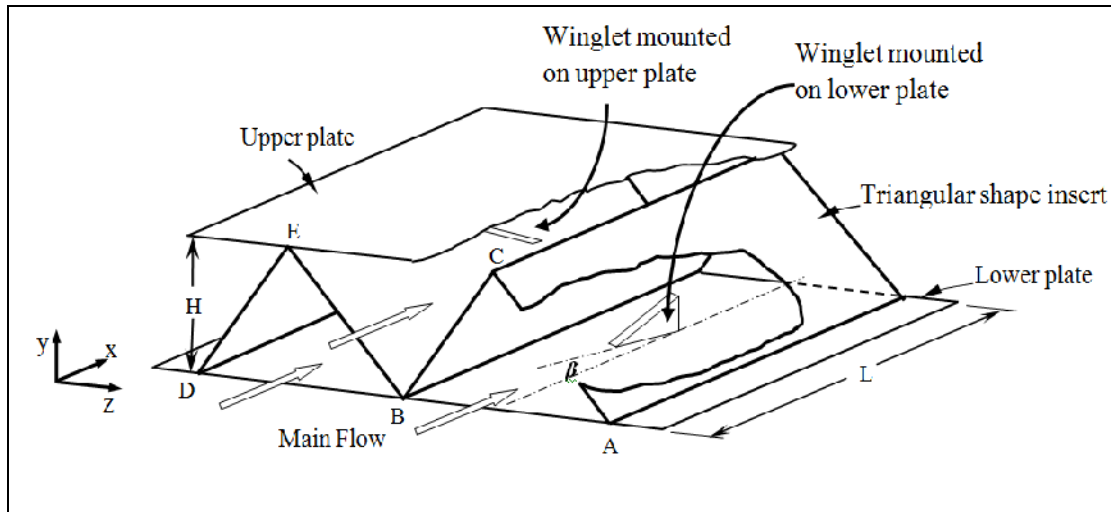


Figure 2 Elaborated view of triangular insert and position of finite thickness winglet
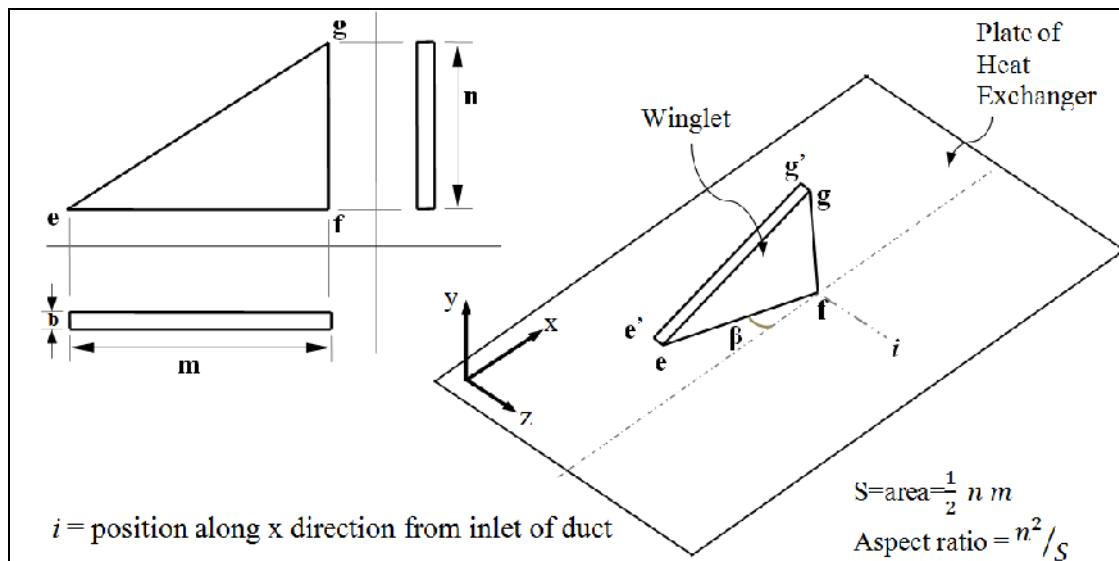on bottom & top plate of heat exchanger



Figure 3 Two dimensional view of finite thickness winglet mounted on the plate

## 2.1. Governing Equations

The present analysis employs the mass continuity, momentum and energy equations expressed in  weak conservative forms. The normalized variables used in the analysis are defined as follows:

Coordinates

$$X = \frac{x}{H} \qquad Y = \frac{y}{H} \qquad Z = \frac{z}{H}$$

Velocities

$$U = \frac{u}{U_{av}} \qquad V = \frac{v}{U_{av}} \qquad W = \frac{w}{U_{av}}$$

Temperature

$$\theta = \frac{(T - T_\infty)}{(T_w - T_\infty)}$$

Time

$$\tau = \frac{t}{H / U_{av}}$$

The aforesaid governing equations are expressed in dimensionless form as follows:

Continuity Equation

$$\frac{\partial U}{\partial X} + \frac{\partial V}{\partial Y} + \frac{\partial W}{\partial Z} = 0 \qquad\qquad (1)$$

Momentum Equation

$$\frac{\partial U}{\partial \tau} + \frac{\partial U^2}{\partial X} + \frac{\partial UV}{\partial Y} + \frac{\partial UW}{\partial Z} = -\frac{\partial P}{\partial X} + \frac{1}{Re}\left[\frac{\partial^2 U}{\partial X^2} + \frac{\partial^2 U}{\partial Y^2} + \frac{\partial^2 U}{\partial Z^2}\right] \qquad\qquad (2)$$

$$\frac{\partial V}{\partial \tau} + \frac{\partial VU}{\partial X} + \frac{\partial V^2}{\partial Y} + \frac{\partial VW}{\partial Z} = -\frac{\partial P}{\partial Y} + \frac{1}{Re}\left[\frac{\partial^2 V}{\partial X^2} + \frac{\partial^2 V}{\partial Y^2} + \frac{\partial^2 V}{\partial Z^2}\right] \qquad\qquad (3)$$

$$\frac{\partial W}{\partial \tau} + \frac{\partial UW}{\partial X} + \frac{\partial VW}{\partial Y} + \frac{\partial W^2}{\partial Z} = -\frac{\partial P}{\partial Z} + \frac{1}{Re}\left[\frac{\partial^2 W}{\partial X^2} + \frac{\partial^2 W}{\partial Y^2} + \frac{\partial^2 W}{\partial Z^2}\right] \qquad\qquad (4)$$

Energy Equation

$$\frac{\partial \theta}{\partial \tau} + \frac{\partial U\theta}{\partial X} + \frac{\partial V\theta}{\partial Y} + \frac{\partial W\theta}{\partial Z} = \frac{1}{Re \cdot Pr}\left[\frac{\partial^2 \theta}{\partial X^2} + \frac{\partial^2 \theta}{\partial Y^2} + \frac{\partial^2 \theta}{\partial Z^2}\right] \qquad\qquad (5)$$

*2.2 Numerical Implementation*
The mesh generated for the computational domain is in the form of Cartesian cells as shown in Figure 4. Unlike the conventional grid, a staggered grid is used here. The nodes pertaining to velocities are located at the centers of the cell faces normal to the respective velocity components and the nodes for pressure and temperature are taken at the center of the cell itself. The axial flow is assumed at the entrance of the duct i.e. V = 0, W = 0 and U = $U_{av}$ = 1.0. The fluid considered is the viscous fluid causing the velocities at all the no-slip surfaces of the triangular domain to be zero i.e. U =0, V =0 and W =0. The surface of the delta winglet is also a no-slip plane and hence, the velocities are zero on the winglet surface. The plane of the winglet passes through the *U* and *W* velocity points of the staggered grid. The velocity *V* is symmetric across the

plane for computation i.e. $U = 0$, $W = 0$ and $V$ is symmetric. The isothermal boundary condition is assumed on all the surfaces of the triangular domain although the slant surfaces are not in direct contact with the hot fluid. To obtain the numerical solution of the Navier-Stokes equations, a modified version of the MAC method by Harlow, F. H. and Welch 1965 is used. Convective term of the Navier-Stokes equations are discretized using weighted average of second upwind scheme by Hirt, C. W., 1975. The diffusive terms are discretized by central difference scheme. After obtaining the velocity field and pressure correction, the energy equation is solved using successive over relaxation technique to determine the temperature field. For the numerical implementation of the current problem, a computer code has been developed in Visual-FORTRAN.
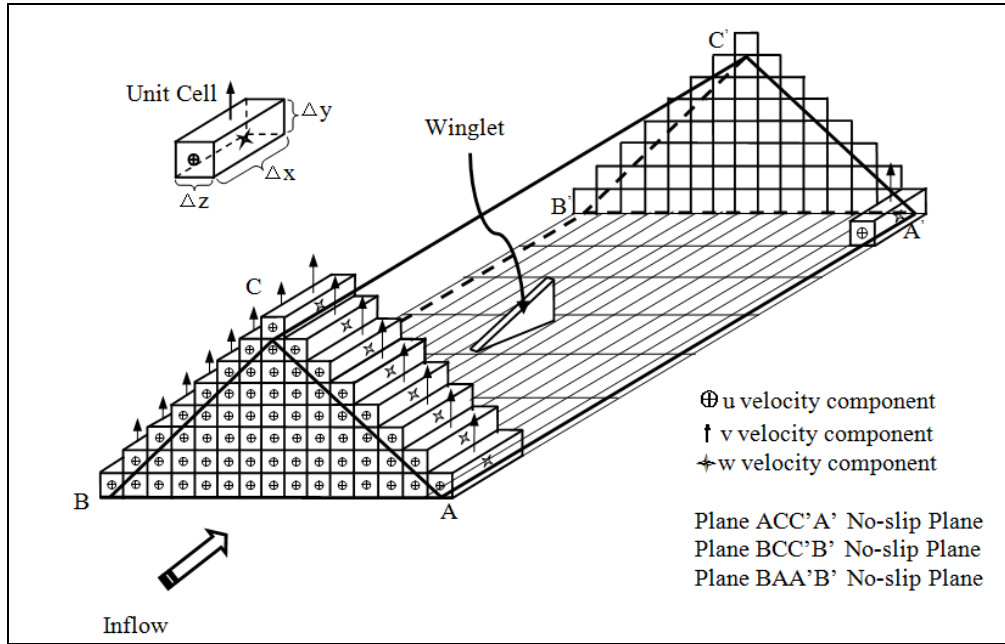


Figure 4 Computational domain with staggered grid mesh showing the location of velocity components

To ensure the smooth transition at the outlet, boundary conditions given by Orlanski 1976 is used

$$\frac{\partial \phi}{\partial \tau} + u_{av} \frac{\partial \phi}{\partial x} = 0 \qquad (6)$$

The MAC algorithm explicitly predicts the flow variables, therefore, the time increment considered is the minimum of the  t's obtained from Courant-Friedrichs-Lewy 2002 condition i.e. equation 7 and the restriction on the basis of grid-Fourier number i.e. equation 8:

$$\delta t < \min \left\{ \frac{\delta x}{|u|}, \frac{\delta y}{|v|}, \frac{\delta z}{|w|} \right\} \qquad (7)$$

$$\delta t < \frac{1}{2} \cdot \frac{\left( \delta x^2 \ \delta y^2 \ \delta z^2 \right)}{\left( \delta x^2 + \delta y^2 + \delta z^2 \right)} \qquad (8)$$

# 3. RESULTS AND DISCUSSION

The range of various parameters considered in the present analysis are specified in Table no. 1

<div align="center">

**Table. 1**

| | |
|---|---|
| Reynolds number, *Re* | 150 to 350 |
| Prandtl number, *Pr* | 0.71 (as for air) |
| angle of attack of vortex generator, | 27$^o$ |

</div>

## *3.1. Flow Visualization*

Figure 7 shows the instantaneous u-z vorticity contours computed numerically at j=0.35 in the duct near winglet for different thickness values at Re=150. Three instantaneous velocity contours are shown in figure 7 for incresing non dimesional thickness of winglet i.e. c/2H= 0.0, 0.025 and 0.05 respectivaly. With increasing thickness of winglet, the flow separates at the leading edge thus forming small recirculation region on front right of the leading edge face. This is due to winding at the frontal blockage area of winglet. Under the influence of cross stream buoyancy, the strength of vortex formed at the trailing edge of the wingletand becomes stronger with increasing winglet thickness. The vortex that is formed on the right side downstream grows with increasing thickness of winglet and thus breaks off the boundary layer deeply near the slant and plate fin surface of the duct.
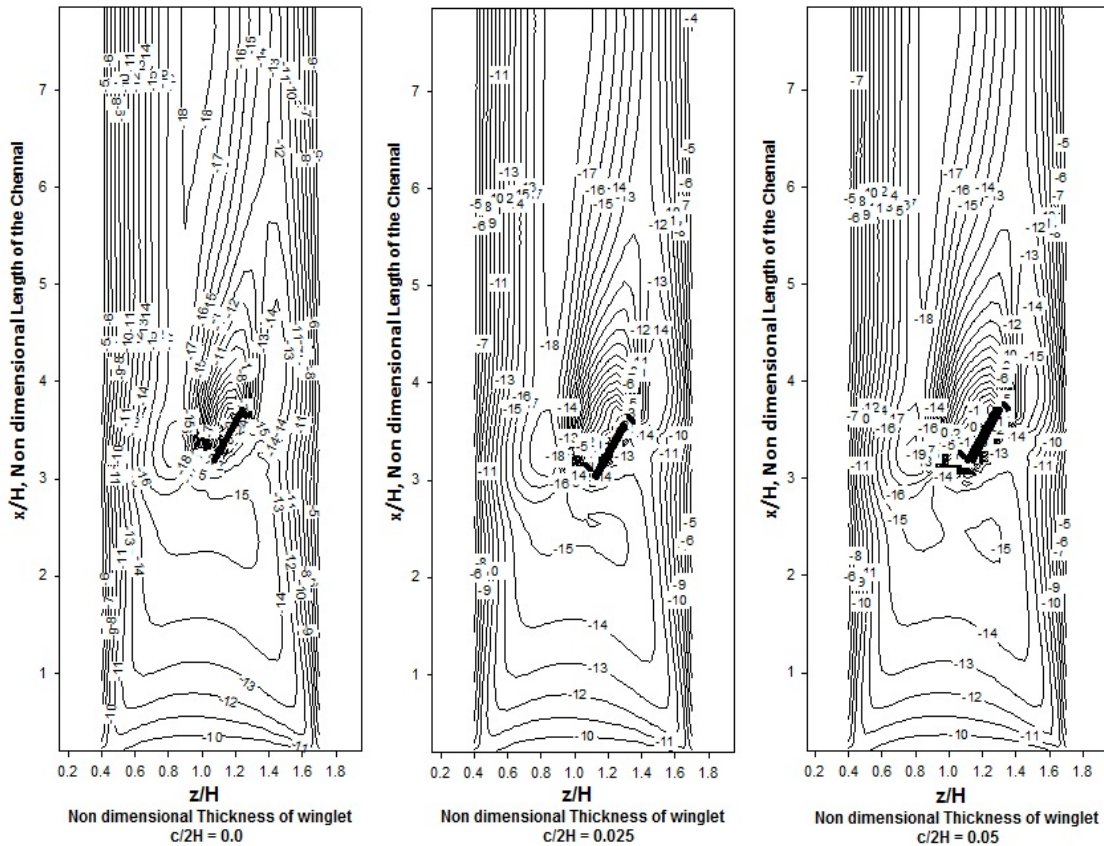


Figure 7 Instantaneous streamlines in the triangular duct passing through winglet under the influence of verging thickness of VG at j= 0.35, Re=150 (Computational Results)

*3.2. Spanwise average Nusselt number*

As the efficacy of heat transfer is characterized by the Nusselt number, its spanwise average value is computed by averaging the local Nusselt number values all around the periphery as follows:

$$Nu_{sa} = \left(\frac{H}{k\,P}\right) \times \left\{ \frac{\left(\int_{p} dP\right)}{\left[(T_{b}(x)) - (T_{w}(x))\right]} \right\} \tag{9}$$

Nussult number is calculated on all three inner wall of the test duct at each longitudinal location. Figure 9 shows the relationship between $Nu_{m}/ Nu_{o}$ and Reynolds number, where $Nu_{m}$ and $Nu_{o}$ are the mean values of spanwise average Nussult number in a complete duct with and without winglet respectively.

Computations carried out for the delta winglet type vortex generator mounted at the position $Xi= 2.765$ from leading edge; (a) the thickness of winglet kept constant and Reynolds number varied; (b) flow parameters (i.e. Reynolds number) kept constant and non-dimesinal thickness c/2H varied. When the non-dimensional thickness of vortex generator kept constant and as the Reynolds number varies, Figure 9 clearly shows an enhancement of 12.91% in the heat transfer rate (i.e., $Nu_{m}/ Nu_{o}$) on increasing the winglet thickness from c/2H=0.0 to c/2H= 0.05.
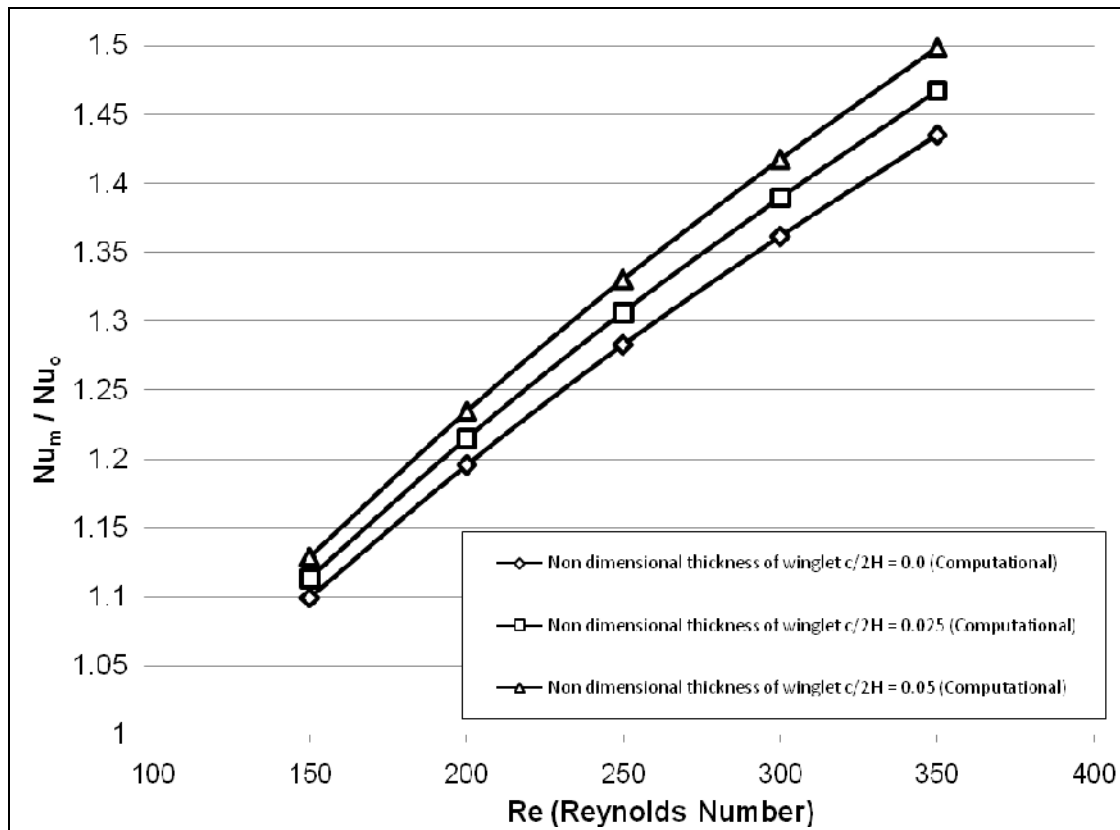


Figure 9 Variation of Nussult Number under the influence of non
dimesional thickness (Computational Results)

### 3.3. Pressure Loss Penalty in terms of Friction Factor

$$f = \frac{C}{R_H} \qquad (10)$$

The pressure drop in the duct system, attributed to fluid friction, is usually computed in terms of friction factor. Figure 10 compares the variation of friction factor with Reynolds Number. With the increase in fin thickness, the friction factor (i.e. pressure drop) increases quite imprecisely. This occurs due to the form drag caused by the pressure difference between the front and rear sides of the vortex generator. Further, the wake width depends on the fin thickness and the boundary layer thickness. The increase in VG thickness increases the wake width and the recirculation regions are wider. The pressure penalty in terms of friction factor is found to be 1.267% for an increase in non dimensional thickness of winglet c/2H from 0.00 to 0.025.
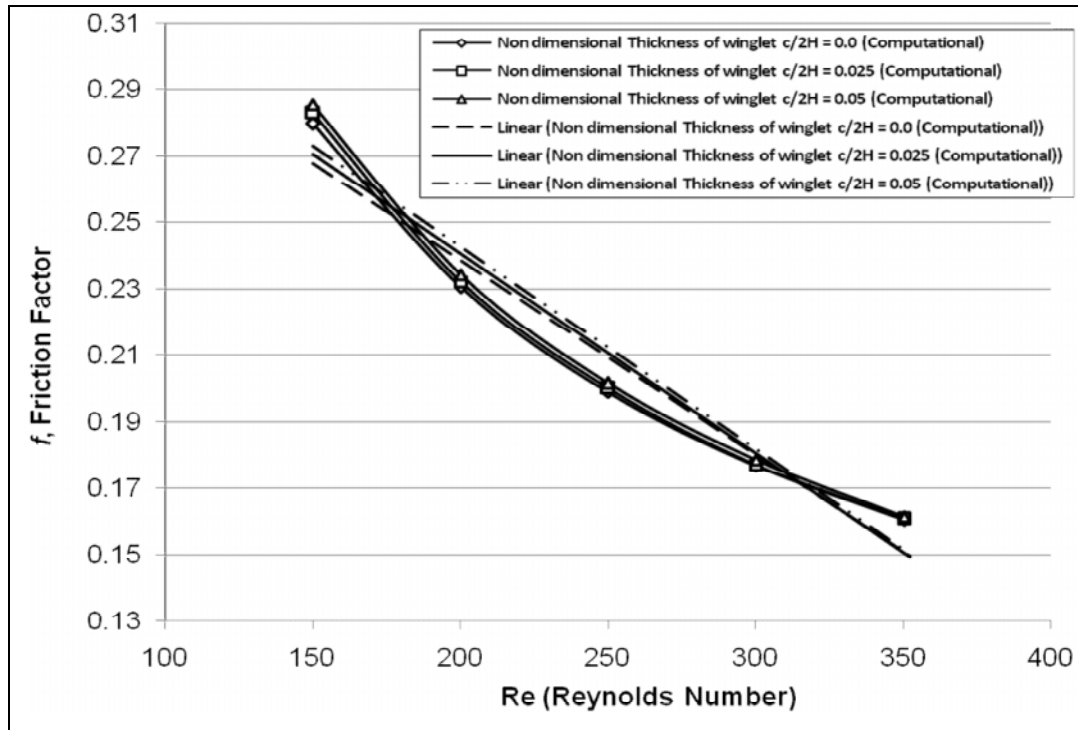


Figure 10 Variation of Friction factor Vs Reynolds Number under the influence
of VG thickness (Computational Results)

### 3.4. Bulk Temperature

As the working fluid flows through the exchanger with or without a winglet, its mean bulk temperature undergoes an increase which is a direct measure of the thermal energy exhcanged during the process. Therefore, it is one the prameters of present study and the following equation is used for its computation:

$$\theta_b(x) = \left\{ \frac{\left( \int_{A_p} |U| \theta \right)}{[(T_b(x)) - (T_w(x))]} \right\} \qquad (11)$$

It can be seen from Figure 11 that as the fluid stream moves axially from x=2.765 to x=3.556, the value of the bulk temperature increases with increasing thickness of the winglet. Due to the spiraling structure of the flow behind the winglet, the cold stream in the core region mixes with the hot fluid from the wall side and hence, the core temperature rises in the downstream region as apparent from Figure 11.
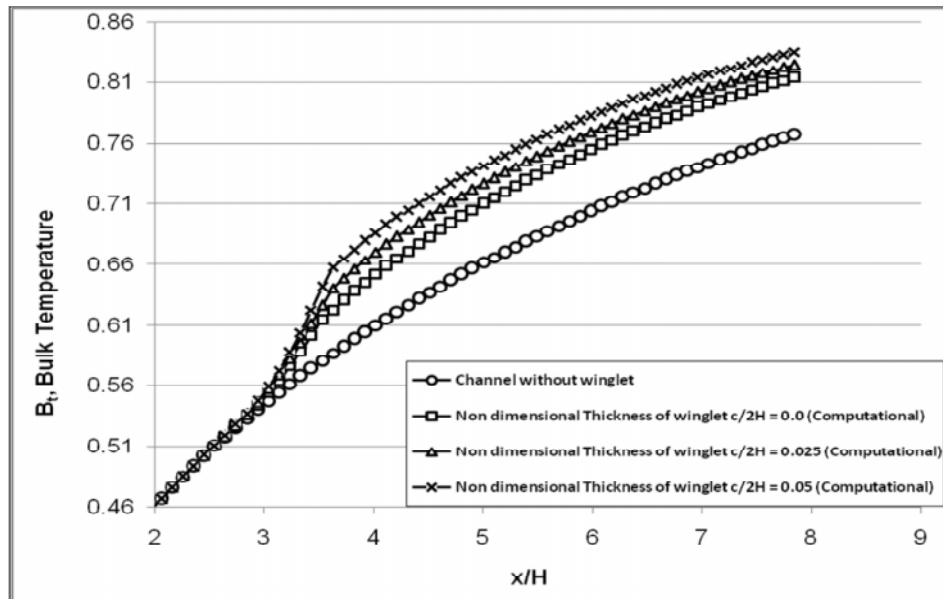


Figure 11 Variation in Bulk temperature along the length of duct under
the influence of winglet thickness (Computational Results)

Figures 12(a) and (b) show the variation of u-component of velocity with respect to time at $x_i$=3.728 so as to ensure the stability of flow behind the winglet type vortex generator. It can be seen that after 25000 time steps, the u-component of velocity appears to be almost stabilized.
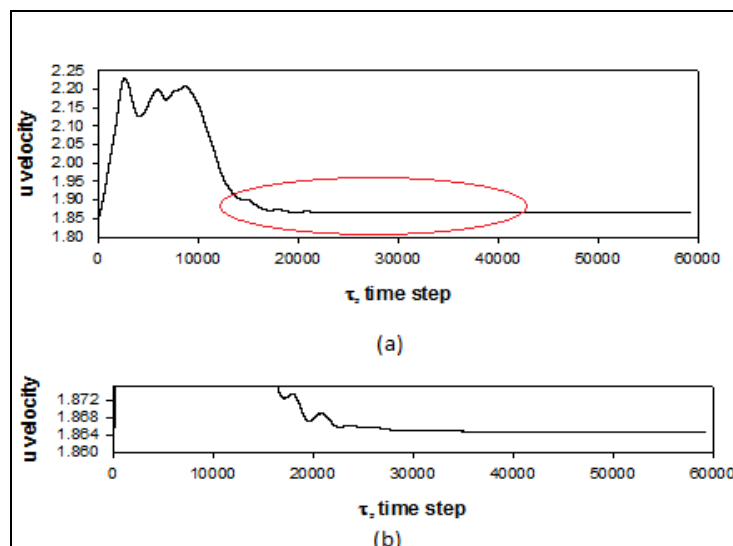


Figure 12 (a) & (b) u velocity fluctuation behind the winglet at non dimesional thickness
c/2H= 0.05 and Re 350 (Computational Results)

After critical examination by reducing the scale, it is found that complete stabilization takes place after 36000 time steps. Finally, it may be concluded that the flow field becomes computationally stable behind the vortex generator at an angle of attack equal to 27$^o$ and Re = 350 for a VG thickness of c/2H = 0.05.

### 3.5. Colburn j factor

The computed results are compared with the measurements taken on the experimental setup for small cross flow plate fin heat exchanger with triangular fins as inserts. The performance of delta winglet is evaluated for laminar flow against the plane duct. Here the parameters of interest is Colburn *j* factor as it is widely used in industries to characterize the heat transfer performance and suitability for specific duties. It is defined as the ratio of convection heat transfer (per unit duct surface area) to the amount virtually transferable (per unit of cross-sectional flow area):

$$j = \left\{ \frac{Nu}{\mathrm{Re}_{D_e} \cdot \mathrm{Pr}^{1/3}} \right\} \qquad (10)$$

Figure 13 shows the Colburn j factor as a function of the airside Reynolds number. It is quite apparent that as the Reynolds number is increased, the heat transfer performance increases in a non-linear fashion which is typical of this class of heat exchangers. The average increase in Colburn J factor over the range of Reynolds number considered is found to be 2.996% for an increase in winglet thickness c/2H from 0.00 to 0.025.
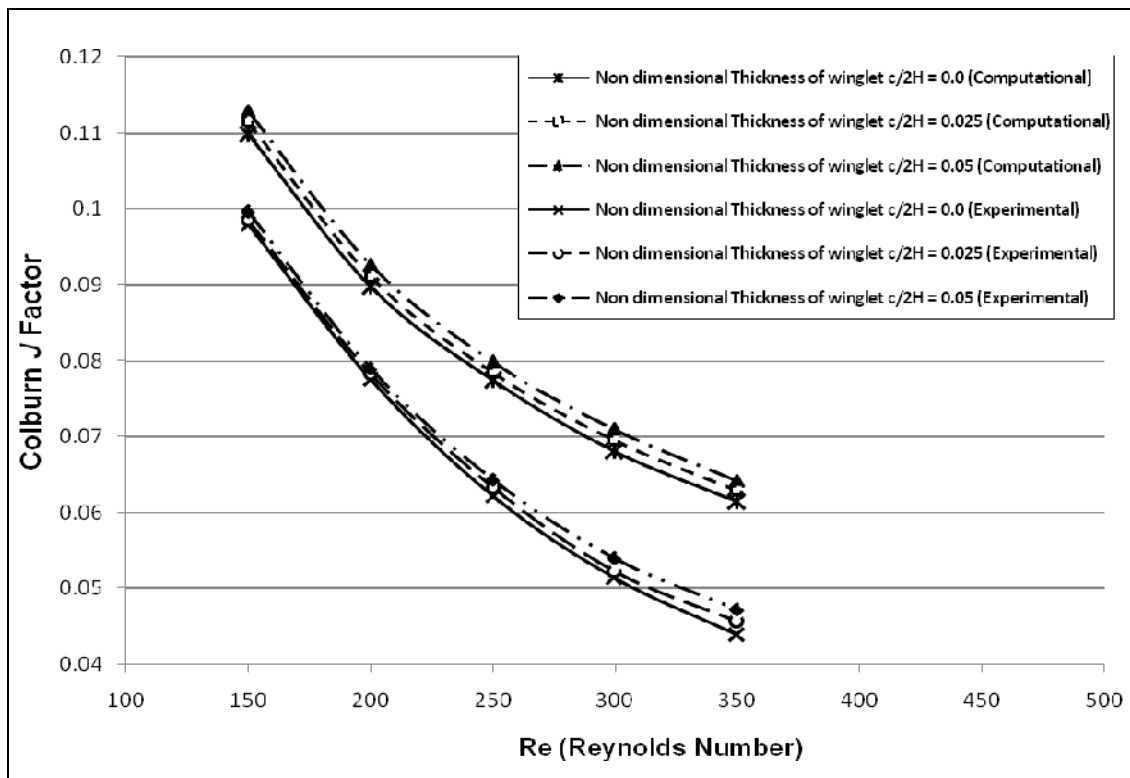


Figure 13 Thermal performances shown with Colburn *j* factor plotted against air-side Reynolds Number
(Computational & Experimental Results)

## 4. CONCLUDING REMARKS

The steady flow in a triangular duct with winglet type vortex generators of non-zero thickness has been investigated numerically and experimentally. The numerical simulations are carried out for three dimensional laminar flow (150 Re 350) with Pr=0.7 (air). With increasing nondimensional thickness of winglet, the blockage ratio in the triangular duct is found to increase and the boundary layers on both slant and bottom surface undergo significant thinning due to acceleration. An enhancement of vortex strength is observed due to thickening of the winglet. Consequently, the interaction between the colder and hotter fluids increases leading to a substantial enhancement (33.15%) in the value of Nussult number. However, an adverse side-effect of winglet is the increase in shear stress values at the duct walls leading to a 2.67% pressure drop for an increase in nondimensional thickness of winglet by c/2H=0.025. The boost in thermal performance quantified in terms of Colburn J factor is found to be 2.996% for the aforesaid increse in nondimensional thickness of winglet.

For the present computational domain, the winglet thickness was limited up to c/2H=0.05 as a thicker winglet may act as a bluff body leading to more wakes and unstable flow.

## 5. REFERENCES

1. Biswas et al., (1996). Numerical and Experimental Determination of Flow Structure and Heat Transfer Effects of Longitudinal Vortices in a Channel flow. *International Journal of Heat and Mass Transfer*, 39, pp. 3441–3451.
2. Brockmeier, U., Guentermann, T .H., Fiebig, M., (1993) Performance Evaluation of a Vortex Generator Heat Transfer Surface and Comparison with Different High Performance Surfaces, *International Journal of Heat Mass Transfer*, Vol-36, pp. 2575-2586.
3. Deb, P., Biswas, G., Mitra, N.K., (1995). Heat Transfer and Flow Structure in Laminar and Turbulent Flows in a Rectangular Channel with Longitudinal Vortices. *International Journal of Heat Mass Transfer*, 38, pp. 2427-2444.
4. Fiebig, M. & Mitra, N.K., (1998). Experimental and Numerical Investigation of Heat Transfer Enhancement with Wing-type Vortex Generators. *International series on Development in Heat Transfer; Computer simulations in Compact Heat Exchangers, Computational Mechanics Publication, USA*, 1, pp. 227-254.
5. Gupta, M., Kasana, K.S., Vasudevan, R., (2009). Numerical Study of Effect on Flow Structure and Heat Transfer with a Rectangular Winglet Pair in a Plate-Fin Heat Exchanger. *Journal of Mechanical Engineering Science, I MechE U.K.*, 223, pp. 2109-2115.
6. Harlow, F. H. and Welch, J. E., (1965). Numerical Calculation of Time-Dependent Viscous Incompressible Flow of Fluid with Free Surfaces. *The Physics of Fluids*, 8, pp. 2182-2188.

7. Hiravennavar, S.R., Tulapurkara, E.G., Biswas, G. A., (2007). Note on the Flow and Heat Transfer Enhancement in a Channel with Built-in Winglet Pair. *International Journal of Heat and Fluid Flow*, 28, pp. 299–305.

8. Hirt, C. W., Nichols, B. D., Romero, N. C., (1975). SOLA—A Numerical Solution Algorithm for Transient Fluid Flows, *Los Alamos Scientific Lab Report LA*, pp.5652.

9. Orlanski, I., (1976) A Simple Boundary Condition for Unbounded Flows. *Journal of Computational Physics*, 21, pp. 251-269.241.

10. Kataoka, K., et al., (1977). Heat/Mass Transfer in Taylor Vortex Flow with Constant Axial Flow Rates. *International Journals of Heat Mass Transfer*, 20, pp. 57-63.

11. Pesteei et al., (2005). Experimental Study of the Effect of Winglet Location on Heat Transfer Enhancement and Pressure Drop in Fin-Tube Heat Exchangers. *International Journals of Applied Thermal Engineering*,  25, pp. 1684–1696.

12. Sachdeva, G., Vasudevan, R., Kasana, K. S., (2010). Computation of Heat Transfer Enhancement in a Plate- Fin Heat exchanger with Triangular Inserts and Delta Wing Vortex Generator. *International Journal for Numerical Methods in Fluids*, 63, pp. 1031–1047.

13. Sohankar, A., Davidson, L., (2003). Numerical Study of Heat and Fluid Flow in a Plate-Fin Heat Exchanger with Vortex Generators. *Turbulence Heat and Mass Transfer*, 4, pp. 1155–1162.

14. Tigglebeck et al., (1992). Flow Structure and Heat Transfer in a Channel with Multiple Longitudinal Vortex Generator. *Experiment Thermal and Fluid Science,* 5, pp. 425-436

15. Torri et al., (1989). The Effects of Longitudinal Vortices on Heat Transfer of Laminar Boundary.  *International Journal Series-II JSME*, 32, pp.359-402.

16. Turk, A.Y., Junkhan, G.H., (1986). Heat Transfer Enhancement Downstream of Vortex Generators on a Flat Plate. *Proceedings of the Eighth International Heat Transfer Conference*, 6, pp. 2903–2908.

17. Vasudevan, R., Eswaran, V. and Biswas, G., (2000). Winglet-type Vortex Generators for Plate Fin Heat Exchangers using Triangular Fins (Part-A). *Numerical Heat Transfer, An International Journal of Computation and Methodology*, 58, pp. 533-555.

18. Yang, J. S., Seo, J. K., Lee, K. B., (2001). A Numerical Analysis on Flow Field and Heat Transfer by Interaction between a Pair of Vortices in Rectangular Channel Flow. *Current Applied Physics*, 1, pp. 393-405.

19. Yang, J. S., Lee, D. W., Choi, G. M.,  (2008). Numerical Investigation of Fluid Flow and Heat Transfer Characteristics by Common Flow Up. *International Journal of Heat and Mass* Transfer, 51, pp. 6332-6336.

20. Yanagihara, J.I., Torii, K., (1993). Heat Transfer Augmentation by Longitudinal Vortices Rows. *Experimental Heat Transfer, Fluid Mechanics and Thermodynamics*, 1, pp. 560–567.

21. Zhang, L. Z., (2007). Laminar Flow and Heat Transfer in Plate-Fin Triangular Ducts in Thermally Developing Entry Region. *International Journal of Heat Mass Transfer*, 50, pp. 1637-1640.

22. Zhu, J. X., Mitra, N. K., Fiebig, M., (1993). Effects of Longitudinal Vortex Generators of Heat Transfer and Flow Loss in Turbulent Channel Flows. *International Journal of Heat Mass Transfer*,  36, pp. 2339-2347.

## NOMENCLATURE

| | | | |
|---|---|---|---|
| $D_H$ | Hydraulic diameter | u,v,w | Axial, normal and spanwise component of velocity |
| f | Friction factor | | |
| h | Heat transfer coefficient | U,V,W | Axial, normal and spanwise component of velocity (non-dimensional) |
| H | Characteristic length dimension (vertical distance between the plates) | | |
| | | x,y,z | Axial, normal and spanwise coordinates |
| j | Colburn factor | X,Y,Z | Axial, normal and spanwise coordinates (non-dimensionalised by H) |
| k | Thermal conductivity of the fluid | | |
| L | Non-dimensional Length of heat exchanger | | Thermal diffusivity |
| Nu | Local Nusselt number based on bulk temperature of the fluid | | Angle of attack of the wing |
| | | | Acute angle of the winglet |
| $Nu_{sa}$ | Combine average Nusselt number based on bulk temperature of the fluid | | Temperature (non-dimensional) |
| | | | Time (non-dimensional) |
| | | | Kinematic viscosity of the fluid |
| P | Non-dimensional pressure | **Subscript** | |
| Pr | Prandtl number | av | average |
| q | Heat flux | b | Bulk temperature |
| Re | Reynolds number | m | Mean |
| t | Time | o | Properties in channel without winglet |
| T | Temperature | sa | Spanwise condition of channel walls |
| $U_{av}$ | Average velocity of the fluid at the channel inlet in axial direction | w | Wall |
| | | | Inlet condition of the temperature |
| $U_c$ | Mean channel outflow velocity | | |